Bioactive Coatings of Endovascular Stents Based on Polyelectrolyte Multilayers

Benjamin Thierry,[†] Françoise M. Winnik,[‡] Yahye Merhi,[§] Jim Silver,[||] and Maryam Tabrizian*,[†]

Department of Biomedical Engineering, Mc Gill University, 3775 University Street, Montreal, Qc, H3A 2B4, Canada, Faculté de Pharmacie et département de Chimie, Université de Montréal, C.P. 6128 Succ. Centre ville, Montreal, Qc, H3C 3J7 Canada, Montreal Heart Institute, 5000 rue Belanger Est, Montreal, H1T 1C8, Canada, and Cordis Corporation—Nitinol Devices & Components (NDC), 47533 Westinghouse Drive, Fremont, California 94539

Received June 11, 2003; Revised Manuscript Received August 29, 2003

Layer-by-layer self-assembly of two polysaccharides, hyaluronan (HA) and chitosan (CH), was employed to engineer bioactive coatings for endovascular stents. A polyethyleneimine (PEI) primer layer was adsorbed on the metallic surface to initiate the sequential adsorption of the weak polyelectrolytes. The multilayer growth was monitored using a radiolabeled HA and shown to be linear as a function of the number of layers. The chemical structure, interfacial properties, and morphology of the self-assembled multilayer were investigated by time-of-flight secondary ions mass spectrometry (ToF−SIMS), contact angle measurements, and atomic force microscopy (AFM), respectively. Multilayer-coated NiTi disks presented enhanced antifouling properties, compared to unmodified NiTi disks, as demonstrated by a decrease of platelet adhesion in an in vitro assay (38% reduction; $p = 0.036$). An ex vivo assay on a porcine model indicated that the coating did not prevent fouling by neutrophils. To assess whether the multilayers may be exploited as in situ drug delivery systems, the nitric-oxide-donor sodium nitroprusside (SNP) was incorporated within the multilayer. SNP-doped multilayers were shown to further reduce platelet adhesion, compared to standard multilayers (40% reduction). When NiTi wires coated with a multilayer containing a fluorescently labeled HA were placed in intimate contact with the vascular wall, the polysaccharide translocated on the porcine aortic samples, as shown by confocal microscopy observation of a treated artery. The enhanced thromboresistance of the self-assembled multilayer together with the antiinflammatory and wound healing properties of hyaluronan and chitosan are expected to reduce the neointimal hyperplasia associated with stent implantation.

Introduction

Percutaneous transluminal coronary angioplasty (PTCA) is widely used for the treatment of occlusive blood vessel diseases. Stent implantation, representing as much as 1 000 000 procedures each year, has improved the safety of the procedures and has been shown to reduce restenosis, i.e., the reobstruction of the targeted artery. The reduction of restenosis is attributed to the scaffolding effect of the stent which prevents elastic recoil and constrictive remodeling of the artery.[1] However stent implantation is also associated with an excessive proliferation of vascular smooth muscle cells (SMCs), extracellular matrix synthesis, and a chronic inflammatory reaction which are believed to be initiated by the deep vascular injury and the endothelial cell denudation created during angioplasty and further enhanced by the presence of a foreign metallic device.[1,2] This complication, known clinically as in-stent restenosis, occurs in about 15 to 30% of the procedures.

Two new developments in stent technology show promise in alleviating thrombosis and in-stent restenosis. One approach consists attempting to improve the biocompatibility of stents by modifying their surfaces with less thrombogenic and inflammatory materials. These coatings include inorganic materials such as carbon, or silicon carbide, or biomimetic materials such as phosphorylcholine-modified surfaces.[1,3] Another approach, which has been shown to be particularly effective in lowering SMCs proliferation and significantly delaying in-stent restenosis, is to coat stents with a layer loaded with therapeutic agents, such as Rapamycin or Taxol, which are released gradually at the implantation site.[1,3] These drugs are usually embedded into a polymeric matrix. However, early work with stents coated with biodegradable polymers, such as polyglycolic acid/polylactic acid copolymers, polycaprolactone polyhydroxy(butyrate valerate), and poly(ethylene oxide)/polybutylene terephthalate [PEO/PBTP] as well as nonbiodegradable polymers, such as polyurethane [PUR], silicone [SIL], and poly(ethylene terephthalate) [PETP], were disappointing and indicated that the polymers

* To whom correspondence should be addressed. E-mail: maryam.tabrizian@mcgill.ca.
[†] Mc Gill University.
[‡] Université de Montréal.
[§] Montreal Heart Institute.
[||] Cordis Corporation—Nitinol Devices & Components.

10.1021/bm0341834 CCC: $25.00
Published on Web 10/07/2003

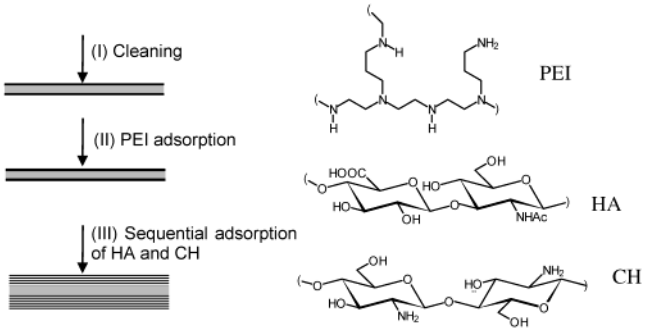

Figure 1. Schematic diagram of the deposition of CH/HA self-assembled multilayer on NiTi substrates; (I) Cleaning of the metallic substrate; (II) Adsorption of a PEI layer; (III) Sequential adsorption of the CH and HA polyelectrolytes. The molecular structures of the polyelectrolytes are presented.

triggered long-term inflammation.[4] The disappointing clinical results recently obtained with the hexanoyltaxol (QP2)-eluting polymer stents (QuaDS) may also be related to such polymer-induced chronic inflammation at the site of stent implantation.[5] This set-back underscores the importance of the biocompatibility of the polymer used as drug carrier material. Other methods to create intelligent biocompatible polymeric interfaces need to be investigated as they may provide relief from the many side effects of stent implantation.

We report here novel coatings for stents created by the formation of insoluble interpolymeric complexes generated by depositing oppositely charged polyelectrolytes. The layer-by-layer self-assembly (L-b-L) of polycations and polyanions into multilayers has emerged as an efficient, versatile, yet simple, technique to create biologically active surfaces. The method relies on the sequential charge inversion of a polymeric surface upon successive immersions of this surface in solutions of oppositely charged polyelectrolytes.[6] The L-b-L technique has been used on various substrates with bioactive molecules, such as drugs, enzymes, DNA, or proteins.[7−13] Bioactive molecules may be incorporated in the multilayer during the polyelectrolyte deposition process, yielding drug-releasing interfaces on various substrates via a process readily applicable to various substrates. We reported recently the deposition of polyelectrolyte multilayers onto angioplasty damaged arteries, resulting in a drastic reduction of thrombogenicity.[14]

We describe the preparation and properties of a new bioactive nanocoating of endovascular devices based on the layer-by-layer self-assembly of two natural polysaccharides, chitosan (CH) and hyaluronan (HA) (Figure 1). Chitosan is a linear polysaccharide containing two β-1,4-linked sugar residus, *N*-acetyl-D-glucosamine and D-glucosamine, distributed randomly along the polymer chain. It is obtained commercially by partial de-*N*-acetylation of chitin. The chitosan used in this study contained approximately 15 mol % *N*-acetyl-D-glucosamine residues. It is only soluble in aqueous solutions of low pH, because its pK_a value is $\sim$ 6.3. Hyaluronan is a naturally occurring linear high molecular weight anionic polymer (pK_a = 2.9) consisting of alternating *N*-acetyl-β-D-glucosamine and β-D-glucuronic acid residues linked (1→ 3) and (1→ 4), respectively (Figure 1). It plays an important structural and mechanical role in various tissues, participates in the control of tissue hydration and water transport, and affects numerous biological processes, such as inflammation, tumor metastasis, and development.[15] The exact role of HA in the fibroproliferative response of vascular vessel toward angioplasty, however, remains unclear and contradictory results have been reported.[16−21] The inhibitive effects of HA with respect to hyperplasia observed after either systemic or local delivery suggest that the antiproliferative effects of HA may be associated with its and antiinflammatory properties.[16] Both CH and HA have found a variety of applications in biomedical engineering and in cardiovascular applications.[22,23] Their use as components of multilayers has been reported in conjunction with oppositely charged polyelectrolytes such as poly(lysine) in the case of HA[24,25] and dextran sulfate in the case of CH.[26]

We describe the deposition of CH/HA self-assembled multilayers on metallic substrates and their characterization by time-of-flight-secondary ions mass spectrometry (ToF−SIMS), atomic force microscopy (AFM), confocal microscopy, and dynamic contact angle measurements. Their antifouling properties are evaluated both in vitro and ex vivo in order to assess whether they may enhance the haemocompatibility of metallic endovascular devices.

To determine if HA/CH multilayers can serve as an in situ drug delivery vehicle, we prepared HA/CH multilayers with sodium nitroprusside (Figure 1), following methodologies previously used to introduce various ionic dyes and proteins within polyelectrolyte multilayers.[27,28] Sodium nitroprusside, a nitrous oxide donor which spontaneously decomposes in biological environments,[29] is widely used clinically to reduce blood pressure and has emerged as a promising modality in the treatment of restenosis.[30] The success of the NO-based therapies seems to rely on the efficiency of the delivery of therapeutic amounts of NO to the vascular wall. We monitored the effect of SNP incorporation on the physicochemical properties of the multilayers, to ensure that SNP incorporation did not affect the creation of a multilayer, and we assessed the level of platelet adhesion onto CH/HA-coated surfaces in order to gain insight into the possible beneficial clinical effects against in-stent restenosis of a strategy combining the complexation of natural polysaccharides and the in situ release of a drug incorporated within the polysaccharide multilayers.

Experimental Section

Substrate Preparation. NiTi disks and wires (Ni: 55.8 wt %) provided by Nitinol Devices & Components (Fremont, CA) were used as substrates. The specimens were polished mechanically to a mirror-like finish using a 0.3-μm alumina paste (disks) or sand-blasted (wires). They were passivated as recommended by ASTM standard.[31] They were subsequently thoroughly cleaned using 2-propanol and pure water. Hydrophobic high-density polyethylene, HDPE, (medical grade) was used as substrate for the dynamic contact angle measurements.

Preparation of the Self-Assembled Coatings. Solutions of sodium hyaluronate (HA, molecular weight 600 000 Da, supplied by Hyal, Canada; 1 mg/mL in 0.14 M aqueous

NaCl, pH 6), chitosan (CH, high molecular weight, deacetylation degree >85%, obtained from Sigma Chemicals; 1.5 mg/mL in 0.1 M acetic acid containing 0.14 M NaCl, pH 4), and polyethyleneimine (PEI, branched, molecular weight 70 000 Da, supplied by Aldrich; 5 mg/mL in 0.14 M aqueous NaCl) were prepared separately. Ultrapure water (18.2 MΩ·cm^2) was used in all experiments (Milli Q system, Millipore). The substrate was dipped in the PEI solution and was allowed to adsorb on the surface for 20 min, thus creating a precursor layer to initiate the L-b-L self-assembly. The multilayer build-up was accomplished by sequential dipping of the substrate in the polysaccharide solution (alternating between HA and CH), followed by a 5-min adsorption and a wash with a flow of 0.14 M NaCl (pH 6). (Figure 1).

HA Derivatives Used for Characterization. Diethylenetriaminopentaacetic acid (DTPA), a chelator able to form stable complexes with radionuclides, was linked to HA as previously described to prepare HA-DTPA with a degree of substitution of ~0.15 DTPA/disaccharide unit.[32] Radiolabeled ^{111}In−HA was prepared as follows: HA-DTPA (29 mg) was dissolved in water (20 mL) for 24 h in a glass vial. Then $^{111}InCl_3$ (100 μCi) was introduced in the vial. The resulting solution was stirred at RT for 2 h to ensure complete complexation. The ^{111}In−HA complex was purified by extensive dialysis against water. The final volume was adjusted to obtain a ^{111}In−HA concentration of 1 mg/mL (0.8 10^6 cpm/mg HA).

The fluorescein derivative of HA (HA-FITC) was used to monitor the fate of the polymer deposited on the stent when placed in contact with an artery. It was prepared as follows. A solution of FITC from Sigma (4 mg, COOH/Fluorescein molar ratio: 25:1) was added to a solution of HA (80 mg) in aqueous borate buffer (pH 9.4). The reaction mixture was stirred at RT for 3 h under N_2 in the dark. HA-FITC was purified by dialysis against borate buffer for 12 h and against water for 3 days. It was recovered by lyophilization.

The HA derivatives, ^{111}In−HA and HA-fluorescein dichlorotriazine (HA-FITC), were used as described above to characterize the build up of the multilayer.

Sodium Nitroprusside Loading. An aliquot of a stock solution of SNP in water (10 mg/mL) was added to the chitosan coating solution 10 min before beginning the coating procedure to achieve a concentration of 0.2 mol SNP/mol NH_2. The multilayered self-assemblies were built up as described above using the chitosan-SNP solution, instead of a CH solution. All manipulations were done in the dark to prevent decomposition of the SNP.

Characterization. Contact angles were obtained from static contact angle measurements of deionized water droplets. Contact angles of a NiTi surface coated with various numbers of CH/HA layers[33] were measured with a video contact angle system (VCA 2500, AST, Billerica, Ma) applying a 1-μL droplet of deionized water (18.2 MΩ) on the samples' surfaces. The contact angles were determined semi-manually from the droplet image with a precision of ±2°.

Time-of-flight secondary ions mass spectrometry analyses were recorded using an ION TOF IV spectrometer (ION-TOF, Germany) equipped with a primary ion Ga^+ beam operated at 15 keV. Areas of about 100 and 8 μm^2 were analyzed under the so-called "static" condition with ion doses of about 10^9 ions/cm^2. The calibration of the mass spectra in the positive mode was based on hydrocarbon peaks such as CH_3^+, $C_2H_2^+$, and $C_3H_5^+$ and peaks from the metallic substrates when possible. Relative normalized intensities [$I_{coatings}/(I_{Ti} + I_{Ni})$] were determined by dividing the integral of the coating characteristic peaks by the integral of the titanium and nickel peaks originating from the substrate. Chemical imaging of the masses associated with CH_3CO^+ (43.017), Ti (47.054), and Ni (57.936) was achieved in the burst alignment mode.

Atomic force microscopy analyses were used to further investigate the growth of the coating on mechanically polished NiTi disks. AFM (Nanoscope III, Digital Instruments, Santa Barbara, CA) was performed in the tapping mode to avoid damaging the surface. Areas of about 5 μm^2 were scanned with a scan rate of 0.5 Hz.

Translocation of the Coating from the Metal Surface to the Vascular Wall. The fluorescence of HA-FITC was used to visualize the presence of the polysaccharide coating onto the metallic substrate and to determine its fate when placed in contact with vascular tissues. The specimens were kept in the dark during all of the experiments to prevent photobleaching. HA(CH/HA)$_4$ multilayers were deposited onto NiTi wires and kept in PBS for various periods of time before being observed with an Axiovert inverted microscope equipped with an LSM 510 confocal system (Zeiss) or kept for translocation studies. Applying a gentle pressure, multilayer coated wires were placed in contact with the luminal surface of fresh aortic porcine arteries placed in a polycarbonate chamber. Wire-contacting arteries were incubated in PBS for 2 days at 4 °C in the dark. Prior to observation by confocal microscopy, the specimens were snap-frozen in 2-methyl-butane using liquid nitrogen and kept at −80 °C, to prevent drug diffusion during handling and storage. Tissues were microtomed into 10 μm thick sections with a cryostat and mounted onto a glass slide prior to fixation with 4% paraformaldehyde. The sections were imaged. Corrections for the artery autofluorescence were performed using a section of porcine artery not exposed to the fluorescent NiTi wires.

Haemocompatibility. Platelet adhesion was investigated as previously described.[14,34] Briefly, fresh blood (120 mL) was drawn from healthy, medication-free volunteers. The blood was collected in syringes preloaded with acide citrate dextrose (ACD). Platelet rich plasma (PRP) was prepared by centrifugation of the blood at 1800 rpm for 15 min. The PRP was then centrifuged at 2200 rpm for 10 min, and the platelet poor plasma (PPP) was recovered as the supernatant. Platelets were carefully resuspended in citrate buffer and incubated with 250 μCi of $^{111}InCl_3$ for 15 min. The platelets were recovered by centrifugation, resuspended in PPP to a concentration of 2.5 × 10^6 platelets/mL. A freshly prepared ^{111}In-platelet solution (3 mL) was added to polystyrene dishes (Corning Inc.) containing the test materials. Platelet adhesion was allowed to proceed for 60 min with gentle shaking. After incubation, the samples were recovered, washed 4 times with saline and fixed in a 2% glutaraldehyde solution. The amount

Table 1. Contact Angle with Water as a Function of the Number of Layers

self-assembled coating	contact angle
NiTi	67 ± 4
NiTi/PEI	69 ± 3
NiTi/PEI/HA	42 ± 4
NiTi/PEI/HA/CH	39 ± 3
NiTi/PEI/HA/(CH/HA)	40 ± 2
NiTi/PEI/HA/(CH/HA)CH	36 ± 4
NiTi/PEI/HA/(CH/HA)$_2$	33 ± 3
NiTi/PEI/HA/(CH/HA)$_3$	31 ± 5
NiTi/PEI/HA/(CH/HA)$_4$	29 ± 4

of platelets was determined using a gamma counter (1470 Wizard, Wallac, Finland) after correction for background signal and radioactivity decay.

The adhesion of ^{111}In polymorphonuclear neutrophils (PMNs) was investigated using an extracorporeal procedure in ex-vivo perfusion chambers. The radiolabeling, animal surgery, and extracorporeal procedures were performed as previously described.[34,35] Four pigs weighing 28 ± 3 kg were used in the experiments. All procedures followed the American Heart Association guideline for animal research and were approved by the local ethics committee. The extracorporeal shunt consisted of two parallel silicon tubing channel circuits connecting the femoral artery to the perfusion chambers and returning to the femoral vein. Radiolabeled PMNs were re-injected into the animals 1 h before the beginning of the experiments. A home-built parallel plate flow chamber was used. Injured arterial segments from normal porcine aortas were prepared as described previously and were used as control.[35] The perfusion procedure was initiated by a 1-min wash with saline. The blood was allowed to circulate into the extracorporeal circuit for 15 min at a physiological wall shear rate of 424 s^{-1}. The circuit was flushed with saline for 30 s, and the samples were recovered and fixed in 1.5% glutaraldehyde in gamma-counter vials. The total amount of PMNs adsorbed on the surface was calculated knowing the specific activity of blood samples used as reference and using haematology performed prior to each experiment.

Results and Discussion

Preparation and Characterization of the Self-Assembled Coating on Surfaces. The multilayer coating procedure was initiated by the adsorption of a PEI layer onto a substrate, yielding a positively charged surface, subsequently placed in contact, in turn, with a solution of the polyanion HA and a solution of the polycation CH. The multilayer construction was expected to modify greatly the wettability of the substrate. This effect was monitored by measuring the contact angle of a water droplet deposited on the surface (Table 1). Deposition of a layer of PEI and subsequent treatment with a solution of HA resulted in a sharp decrease of the contact angle (42 ± 4 Vs 67 ± 4 for NiTi). The contact angle further decreased with increasing layer number, reaching an angle of about 30° upon deposition of 7 single layers and remaining constant upon further polyelectrolyte layer deposition. In agreement with previously reported data, the fact that, after deposition of 4 bilayers, there was no further changes in the contact angle led us to conclude that at least 4 bilayers were necessary to mask the substrate with respect to the properties of the multilayer/water interface.[36] As a consequence, HA(CH/HA)$_4$ self-assembled coatings built on PEI−NiTi were considered as representative of the 3-dimensional polysaccharide multilayer coating and used in the biological assays described below.

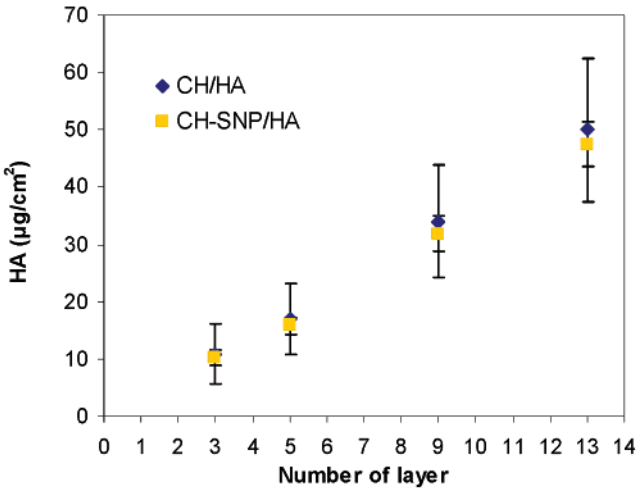

Figure 2. Amount of In^{111}-HA (μg/cm^2) as a function of the number of layer for the CH/HA and CH-SNP/HA polyelectrolytes self-assembled onto NiTi substrates; 3 NiTi-PEI-HA(CH/HA)$_1$, 5 NiTi-PEI-HA(CH/HA)$_2$ and so on.

The multilayer build-up procedure was monitored next by measuring the radioactivity of multilayers obtained using ^{111}In−HA instead of HA. This highly sensitive method allowed us to quantitate the amount of HA deposited in each step and thus to ascertain that the multilayer build-up procedure follows the general L-b-L mechanism. It should be noted that this analytical method gives us information on the construction of ^{111}In−HA/CH multilayers and not on HA/CH assemblies. Data presented elsewhere indicate that the use of the labeled HA slightly overestimates the amount of HA incorporated in the multilayer under the conditions employed in this work.[14] The amount of HA in the coating increased linearly with the number of layers (Figure 2, slope: 3.8 μg HA/bilayer, r^2= 0.99), indicating that the two polyelectrolytes follow a typical linear multilayer construction mechanism.

A more detailed analysis of the nanocoating was obtained by a ToF−SIMS examination of metal surfaces recovered after each coating step. A spectrum of a PEI coated surface presented several nitrogen containing peaks attributed to PEI, e.g., CH_2N^+ (*m/z* 28.018), $C_2H_3N^+$ (*m/z* 41.025), and $C_3H_8N^+$ (*m/z* 58.064) (Figure 2) and also several peaks characteristic of NiTi (^{46}Ti, *m/z* 45.954), (^{47}Ti, *m/z* 46.954), (^{48}Ti, *m/z* 47.954), (^{48}TiH, *m/z* 48.956), (^{50}Ti, *m/z* 45.947), (^{48}TiO, *m/z* 63.949), (^{58}Ni, *m/z* 57.936), (^{58}NiH, *m/z* 58.942), and(^{60}Ni, *m/z* 59.931), suggesting that the metal surface has not been fully coated with PEI. Next, we recorded ToF−SIMS spectra of a HA(CH/HA)$_4$ self-assembled coating (Figure 3). A spectrum of a Si wafer spin-coated with HA was also recorded to allow the attribution of the peaks characteristic of HA. In agreement with a previously reported ToF−SIMS analysis of HA, the spectrum of the HA-coated Si wafer

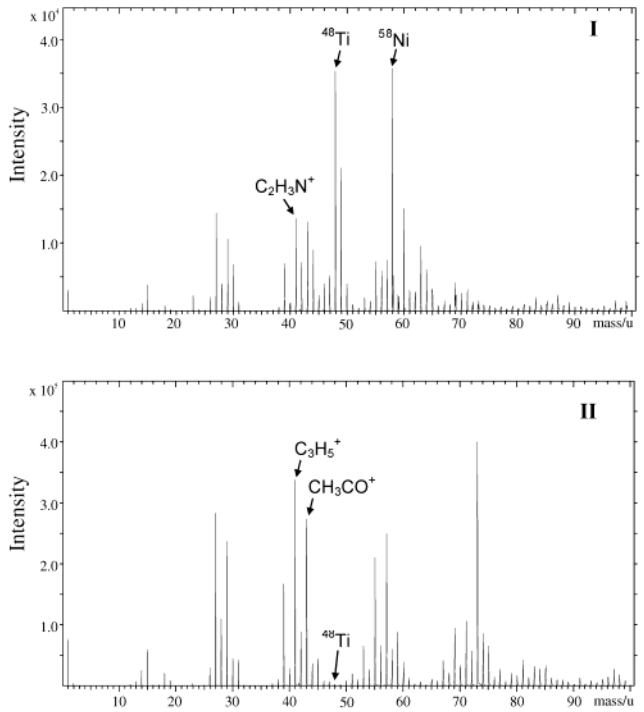

Figure 3. Positive ion ToF SIMS spectra (*m*/*z* 0−100) for (I) PEI modified NiTi and (II) PEI-HA(CH/HA)$_4$ self-assembled coating on NiTi.

Table 2. ToF SIMS Normalized Intensities of the CH_3CO^+ Peak (M/z 43.0174) as a Function of the Number of Layer

self-assembled coating	CH_3CO^+ normalized intensity
NiTi/PEI/HA/(CH/HA)	32
NiTi/PEI/HA/(CH/HA)$_2$	60.9
NiTi/PEI/HA/(CH/HA)$_4$	88.7
NiTi/PEI/HA/(CH/HA)$_6$	296.8
NiTi/PEI/HA/(CH/HA)$_{10}$	No metallic signal detected

presented an intense peak at *m*/*z* 43.017 attributed to the CH_3CO^+ ion from the HA *N*-acetyl.[37] The normalized intensity of the CH_3CO^+ peak increases as a function of the number of layers (Table 2). This peak was used to correlate the quantitative information obtained using the ^{111}In−HA and the ToF−SIMS analyses. In addition to a peak at *m*/*z* 43.0174, the ToF−SIMS spectrum of the HA(CH/HA)$_4$ coated PEI−NiTi (Figure 3) presents hydrocarbon peaks, such as $C_2H_3^+$ (*m*/*z* 27.022), $C_3H_3^+$ (*m*/*z* 39.022), $C_3H_5^+$ (*m*/*z* 41.0375), and $C_4H_7^+$ (*m*/*z* 55.053) as well as oxygen and nitrogen containing peaks, such as CH_4N^+ (*m*/*z*= 30.033), $C_2H_3N^+$ (*m*/*z*= 41.025), $C_2H_2O^+$ (*m*/*z*= 42.099), $C_2H_3O^+$ (*m*/*z*= 43.017), and $C_2H_4NO^+$ (*m*/*z*= 58.027). Peaks due to the metal substrate were still detectable, but their intensity, compared to that of the carbonaceous species, is much weaker than in the spectrum of the PEI−NiTi sample. No ions originating from the metallic substrate were detected on the spectrum of a HA(CH/HA)$_{10}$ multilayer coated NiTi sample.

The uniformity of the self-assembled coating on the scale of a cell, a few μm, was assessed by ToF SIMS imaging of HA(CH/HA)$_4$-coatings. The peak assigned to the CH_3CO^+ peak was employed. Homogeneous chemical images were obtained over an 8 μm^2 area (Figure 4). Chemical mapping of metallic peaks attributed to the substrate was performed

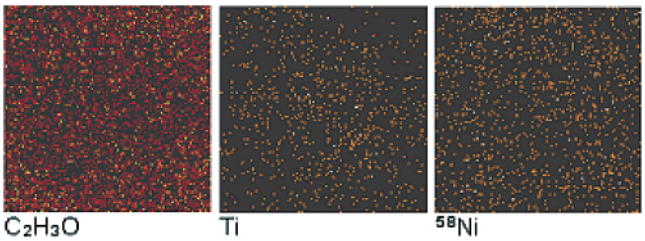

Figure 4. Chemical imaging of a PEI-HA(CH/HA)$_4$ self-assembled multilayer showing the distribution of CH_3CO^+ (43.017), Ti (47.054), and Ni (57.936) ions on the surface (7.9 μm^2).

as well, yielding homogeneous images of much lower intensity (Figure 4). This may be attributed to some degree of porosity of the multilayer coating, possibly resulting from exposure of the multilayers to the ultrahigh vacuum imposed by the SIMS analysis. ToF−SIMS investigation of self-assembled multilayer on Si wafers has also shown that atomic or small molecular ions are less surface sensitive than large molecular ions.[38]

The evolution of surface topography throughout the multilayer construction process was assessed next using atomic force microscopy. Our observations for the sequential deposition onto polished NiTi (I) of PEI−HA(CH/HA)$_2$ (II), PEI−HA(CH/HA)$_5$ (III), and PEI−HA(CH/HA)$_{10}$ (IV) are presented in Figure 5. Note that the naked polished metal surface displays a slightly striated topography, the striations are believed to be caused by the use of a polishing paste consisting of alumina particles ~0.3 μm in diameter. These surface features were gradually masked in the coated surfaces and replaced by nanosized clusters. These structures increase in size with the number of layers, reaching a height of a few tens of nanometers and an average diameter of 250 nm. The original pattern featured in the images of the mechanically polished metal is completely masked by a multilayer coating consisting of 13 layers. The appearance and growth of small globular features in the hundred of nanometers range may be the indication of the formation of complex coacervates, as reported previously in the case of the L-b-L self-assembly of poly(L-lysine) and HA.[25]

One of the objectives of this study was to determine if a L-b-L assembled stent coating can act as a drug reservoir for in situ drug release following stent implantation. To test this hypothesis, an anionic drug, sodium nitroprusside (SNP), was incorporated in the multilayer. It was introduced within the coating during the chitosan deposition step, as the cationic polysaccharide is able to form a complex with SNP by electrostatic interactions. That SNP was incorporated into the coating by this method and that the construction mechanism was not disrupted by the presence of small amounts of SNP was established, by the radiolabeling method described above. No difference was observed in the amount of radiolabeled HA deposited as a function of the number of layers whether the multilayers were constructed with chitosan-SNP or chitosan alone (Figure 2). The ToF SIMS spectrum of an SNP-containing 9-layer assembly exhibited a peak at 55.84 *m*/*z*, a value characteristic of Fe which is present in the structure of SNP, but not in any other component of the coating. Taken together the ToF SIMS data and the radiolabeling experiment confirm that premixing

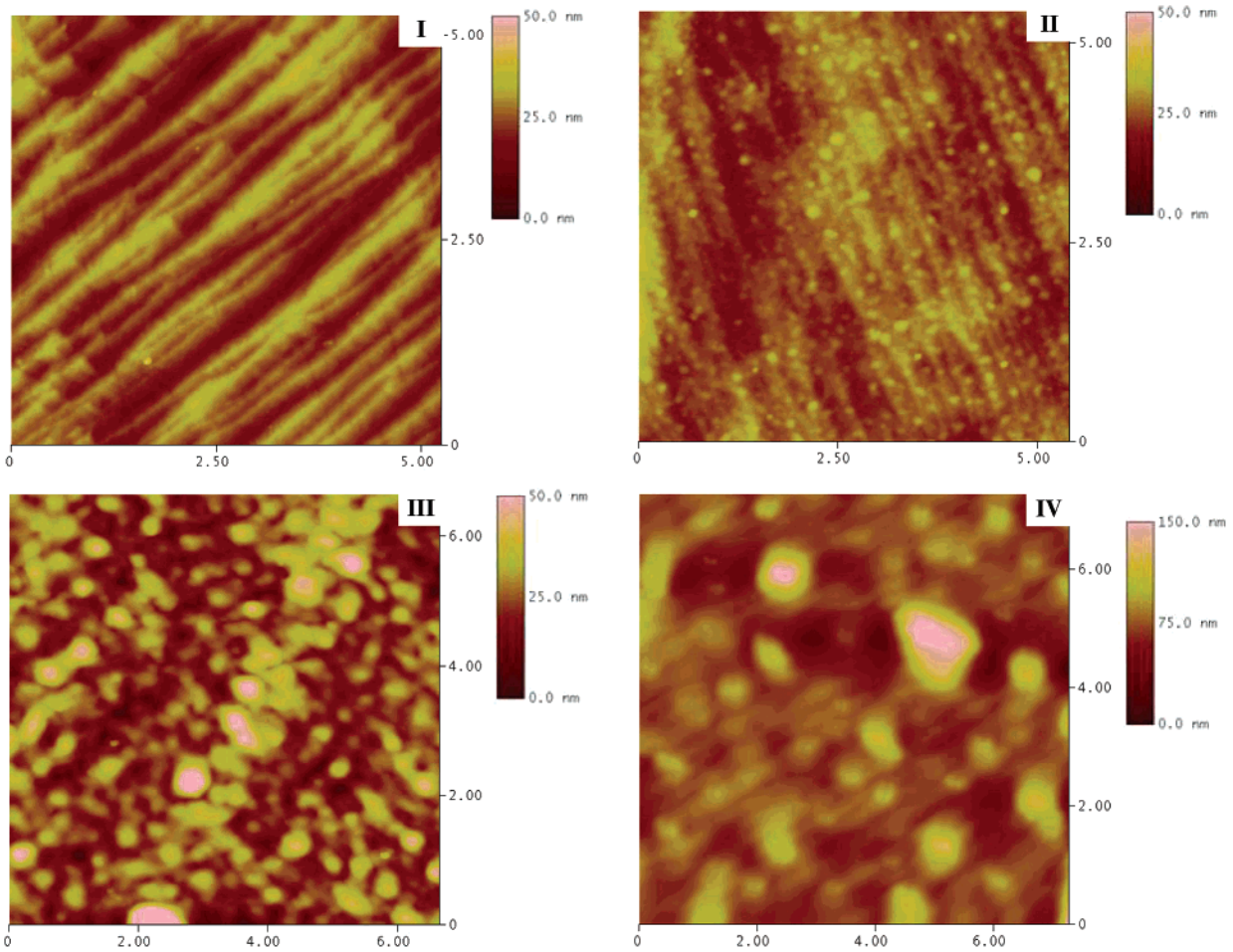

Figure 5. AFM tapping mode height images of (I) the mechanically polished NiTi, (II) PEI-HA(CH/HA)$_2$ coated NiTi, PEI-HA(CH/HA)$_5$ coated NiTi and PEI-HA(CH/HA)$_{10}$ coated NiTi; Z scales are 50 nm for images (I) to (III) and 150 nm for image (IV).

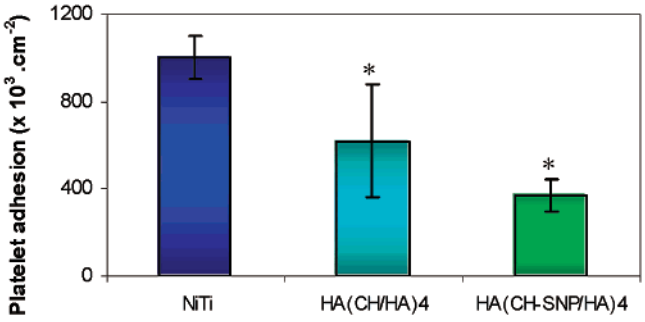

Figure 6. Platelet adhesion on NiTi, NiTi-PEI-HA(CH/HA)$_4$, and NiTi-PEI-HA(CH-SNP/HA)$_4$; $* p < 0.05$ Vs NiTi.

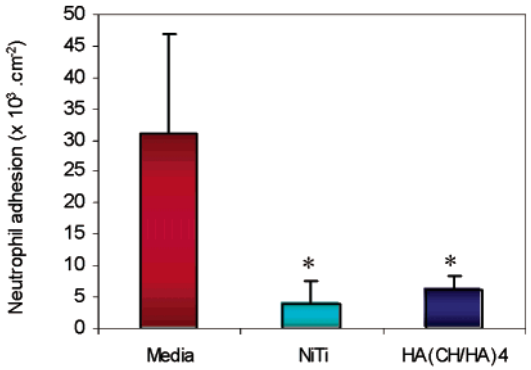

Figure 7. Neutrophil adhesion on damaged artery (Media), NiTi, and NiTi-PEI-HA(CH/HA)$_4$; Mean ± SEM; $* P < 0.05$ vs Media (Student-t-test).

chitosan and SNP does not interfere significantly with the L-b-L construction, vouching for the flexibility of the technique in creating functional surfaces.

Haemocompatibility of CH/HA Coated NiTi Surfaces. The thromboresistance of an HA(CH/HA)$_4$ coated metallic substrate was investigated using an platelet adhesion assay. As depicted in Figure 6, platelet adhesion was significantly reduced by 38% onto NiTi−PEI−HA(CH/HA)$_4$ after 60 min of exposure to platelet rich plasma (619.7 ± 258.0 10^3 platelets/cm^2 versus 1005.9 ± 97.7 10^3 platelets/cm^2 for bare NiTi; $p = 0.036$). The incorporation of sodium nitroprusside within the multilayered coating further decreased platelet adhesion by 40% (371.5 ± 74.5 10^3 platelets/cm^2 for SNP containing HA(CH/HA)$_4$ coated NiTi versus 619.7 ± 258.0 10^3 platelets/cm^2 for HA(CH/HA)$_4$ NiTi; $P = 0.09$). On the contrary, the CH/HA multilayer did not inhibit polymorphonuclear neutrophils (PMNs) adhesion after a 15-min perfusion in a porcine ex vivo assay (Figure 7). In fact, PMN adhesion *increased* slightly onto the coated surface, compared to bare metal (6.1 ± 2.2 10^3/cm^2 vs 3.9 ± 3.8 10^3/cm^2). PMN adhesion on both bare metal and polysaccharide coated metal surfaces was significantly lower than PMN adhesion on the damaged porcine aortic segment used as control (30.9 ± 16.1 10^3/cm^2).

Platelet adhesion is known to be initiated by adsorption of plasma proteins, such as fibrinogen. The antifouling

properties of HA immobilized onto surfaces are well documented. It is believed that they are attributable to the hydration layer surrounding HA molecules on the surface.[39] It is expected that reduction of adhesion and activation of platelets could reduce the proliferative vascular response. Interestingly, the multilayer did not prevent neutrophil adhesion in the ex vivo assays and even slightly increased their adhesion in comparison to bare metal. This is in agreement with previous reports showing adhesion of monocyte and PMN to antifouling hydrophilic surfaces.[40] The neutrophil adhesion could result from nonspecific interactions or from specific adhesion through ligand−receptor mediated interactions such as CD 44 that are expressed on leukocytes. The modest neutrophil adhesion onto polysaccharide multilayer remained however far under the level measured onto damaged arteries.

Ex Vivo Stability of the CH/HA Coating in Contact with a Vascular Wall. A fluorescently labeled HA sample, HA-FITC, was used to monitor the deposition of the multilayer onto the metallic substrate. Fluorescence confocal microscopy observation of HA-FITC-$(CH/HA\text{-}FITC)_4$ coated wires confirmed the uniform presence of HA-FITC on the wire surface, even after the coated wires had been incubated in PBS for several days (Figure 8). A porcine aortic sample was incubated for 3 days in PBS while maintained in contact with the coated wire. The treated artery displayed fluorescence attributed to the transfer of FITC-HA from the coated wire-mesh to the artery surface as a result of contact with the stent.

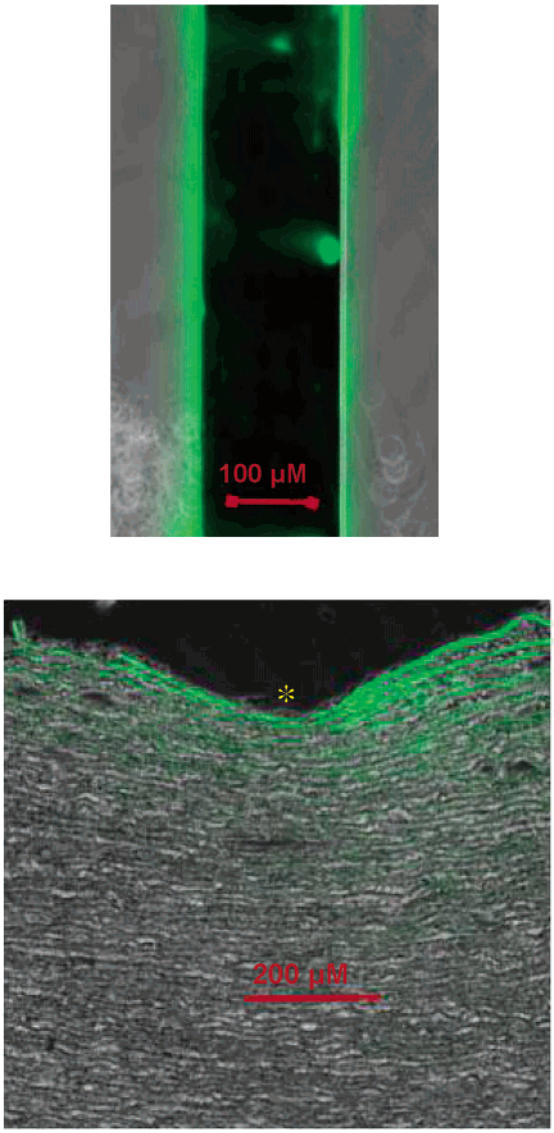

Figure 8. Confocal microscopy images of: (I) PEI/HA-FITC$(CH/HA\text{-}FITC)_4$ coated NiTi wires; (II) Cross-section of a damaged artery maintained in contact with a coated wire for 48 h in PBS showing the presence of HA-FITC translocated from the wire onto the vessel. (*) Groove due to the wire impact on the luminal surface of the artery.

Conclusion

The tremendous potential of the polyelectrolyte multilayer self-assembly methodology to engineer biologically active surfaces lies in its versatility and reproducibility.[6,41] Our study demonstrates that the self-assembled deposition of polysaccharide multilayers can be achieved with excellent control of the growth mechanism and the surface coverage, even in the presence of an added drug. The CH/HA system is characterized by a linear growth as demonstrated using the radiolabeled HA-^{111}In derivative. From contact angle measurements and ToF SIMS analysis of deposited multilayers, we established that a minimum of 4 bilayers were needed to mask the metal substrate from its environment. The hydrogellike surface created by the polysaccharide multilayer enhanced the thromboresistance of the surface, but surprisingly did not reduce PMN adhesion. Platelet adhesion was indeed reduced by 40% in comparison to bare NiTi surfaces which, by themselves, display good haemocompatibility.[34] The multilayer self-assembly used in this study offers an innovative way to achieve 3-dimensional coatings that fully exploit the biocompatibility of natural polysaccharides such as HA and CH. Importantly, the L-b-L technique does not require the use of toxic cross-linking agents, such as glutaraldehyde, which could compromise the biocompatibility of the multilayer coating. Interestingly, placing arterial segments in vitro in contact with multilayer coated wires for several days resulted in the transfer of the polyelectrolytes, or at least HA, from the wire to the tissue. Given the beneficial biological effects of HA, this translocation of HA to the vascular wall may prove advantageous and lead to further reduction of neointimal hyperplasia.

This study also aimed to investigate the potential use of self-assembled structures for the local delivery of bioactive molecules. The incorporation of SNP within the polysaccharide multilayer resulted in a reduction of platelet adhesion, compared to multilayers devoid of drug. This result confirmed the potential of such biocompatible self-assembled structures as therapeutic drug delivery media. Their suitability as host to a variety of biologically active molecules, such as DNA or proteins, offers numerous opportunities for clinical applications.

Acknowledgment. This work was partly supported by NSERC grants and by the Center for Biorecognition system and Biosensors (CBB). We thank Cordis Corporation—Nitinol Devices & Components (Fremont, CA) for their technical and financial support. The authors thank S. Poulin

for her precious technical assistance and useful discussions with ToF SIMS analysis. Thanks also go to J. F. Théoret and N. Jacob from the Montreal Heart Institute for their help in the haemocompatibility assays and P. Cap for manuscript reviewing.

References and Notes

(1) Babapulle, M. N.; Eisenberg, M. J. *Circulation* **2002**, *106* (21), 2734.
(2) Welt, F. G.; Rogers, C. *Arterioscler. Thromb. Vasc. Biol.* **2002**, *22* (11), 1769.
(3) Babapulle, M. N.; Eisenberg, M. J. *Circulation* **2002**, *106* (22), 2859.
(4) van der Giessen, W. J.; Lincoff, A. M.; Schwartz, R. S.; van Beusekom, H. M.; Serruys, P. W.; Holmes, D. R., Jr; Ellis, S. G.; Topol, E. J. *Circulation* **1996**, *94* (7), 1690.
(5) Virmani, R.; Liistro, F.; Stankovic, G.; Di Mario, C.; Montorfano, M.; Farb, A.; Kolodgie, F. D.; Colombo, A. *Circulation* **2002**, *106* (21), 2649.
(6) Decher, G. *Science* **1997**, *277*, 1232.
(7) Chung, A. J.; Rubner, M. F. *Langmuir* **2002**, *18*, 1176.
(8) Qiu, X.; Leporatti, S.; Donath, E.; Mohwald, H. *Langmuir* **2001**, *17*, 5375.
(9) Pei, R.; Cui, X.; Yang, X.; Wang, E. *Biomacromolecules* **2001**, *2* (2), 463.
(10) Lvov, Y. u. M.; Sukhorukov, G. B. *Membr. Cell Biol.* **1997**, *11* (3), 277.
(11) Chluba, J.; Voegel, J. C.; Decher, G.; Erbacher, P.; Schaaf, P.; Ogier, J. *Biomacromolecules* **2001**, *2* (3), 800.
(12) Vazquez, E.; Dewitt, D. M.; Hammond, P. T.; Lynn, D. M. *J. Am. Chem. Soc.* **2002**, *124* (47), 13992.
(13) Lvov, Y.; Lu, Z.; Schenkman, J. B.; Zu, X.; Rusling, J. F. *J. Am. Chem. Soc.* **1998**, *120* (17), 4073.
(14) Thierry, B. J.; Winnik, F. M.; Merhi, Y.; Tabrizian, M. *J. Am. Chem. Soc.***2003**, *125*, 7494.
(15) Abatangelo, G., Weigel, P. H., Eds.; Elsevier: Amsterdam, 2000.
(16) Heublein, B.; Evagorou, E. G.; Rohde, R.; Ohse, S.; Meliss, R. R.; Barlach, S.; Haverich, A. *Int. J. Artif. Organs* **2002**, *25* (12), 1166.
(17) Finn, A. V.; Gold, H. K.; Tang, A.; Weber, D. K.; Wight, T. N.; Clermont, A.; Virmani, R.; Kolodgie, F. D. *J Vasc Res* **2002**, *39* (5), 414.
(18) Travis, J. A.; Hughes, M. G.; Wong, J. M.; Wagner, W. D.; Geary, R. L. *Circ. Res.* **2001**, *88* (1), 77.
(19) Geary, R. L.; Nikkari, S. T.; Wagner, W. D.; Williams, J. K.; Adams, M. R.; Dean, R. H. *J. Vasc. Surg.* **1998**, *27* (1), 96, discussion 106.
(20) Chajara, A.; Raoudi, M.; Delpech, B.; Leroy, M.; Basuyau, J. P.; Levesque, H. *Arterioscler. Thromb. Vasc. Biol.* **2000**, *20* (6), 1480.
(21) Deux, J. F.; Prigent-Richard, S.; d'Angelo, G.; Feldman, L. J.; Puvion, E.; Logeart-Avramoglou, D.; Pelle, A.; Boudghene, F. P.; Michel, J. B.; Letourneur, D. *J. Vasc. Surg.* **2002**, *35* (5), 973.
(22) Chupa, J. M.; Foster, A. M.; Sumner, S. R.; Madihally, S. V.; Matthew, H. W. *Biomaterials* **2000**, *21* (22), 2315.
(23) Morra, M.; Cassineli, C. *J. Biomater. Sci. Polym. Ed.* **1999**, *10* (10), 1107.
(24) Picart, C.; Mutterer, J.; Richert, L.; Luo, Y.; Prestwich, G. D.; Schaaf, P.; Voegel, J. C.; Lavalle, P. *Proc. Natl. Acad. Sci. U.S.A.* **2002**, *99* (20), 12531.
(25) Picart, C.; Lavalle, Ph.; Hubert, P.; Cuisinier, F. J. G.; Decher, D.; Schaaf, P.; Voegel, J.-C. *Langmuir* **2001**, *17*, 7414.
(26) Serizawa, T.; Yamaguchi, M.; Akashi, M. *Biomacromolecules* **2002**, *3* (4), 724.
(27) Das, S.; Pal, A. J. *Langmuir* **2002**, *18*, 458.
(28) Ariga, K.; Onda, M.; Lvov, Y.; Kunitake, T. *Chem. Lett.* **1997**, 25.
(29) Wang, P. G.; Xian, M.; Tang, X.; Wu, X.; Wen, Z.; Cai, T.; Janczuk, A. J. *Chem. Rev.* **2002**, *102* (4), 1091.
(30) Provost, P.; Merhi, Y. *Thromb. Res.* **1997**, *85* (4), 315.
(31) *Annual Book of ASTM Standards: Medical Devices and Services*; American Society for Testing and Materials: West Conshohocken, PA, 1995; Vol. 13.01, p 6.
(32) Gouin, S.; Winnik, F. M. *Bioconjugate Chem.* **2001**, *12* (3), 372.
(33) In this work, "layer" refers to the increment in thickness after exposure to one of the polyelectrolyte solution.
(34) Thierry, B.; Merhi, Y.; Bilodeau, L.; Trépanier, C.; Tabrizian, M. *Biomaterials* **2002**, *23* (14), 2997.
(35) Merhi, Y.; King, M.; Guidoin, R. *J. Biomed. Mater. Res.* **1997**, *34* (4), 477.
(36) Chen, W.; McCarthy, T. J. *Macromolecules* **1997**, *30* (1), 78.
(37) Shard, A. G.; Davies, M. C.; Tendler, S. J. B.; Bennedetti, L.; Purbrick, M. D.; Paul, A. J.; Beamson, G. *Langmuir* **1997**, *13*, 2808.
(38) Delcorte, A.; Bertrand, P.; Arys, X.; Jonas, A.; Wischerhoff, E.; Meyer, B.; Laschewsky, A. *Surf. Sci.* **1996**, *366*, 149.
(39) Morra, M. *J. Biomater. Sci. Polym. Ed.* **2000**, *11* (6), 547.
(40) DeFife, K. M.; Shive, M. S.; Hagen, K. M.; Clapper, D. L.; Anderson, J. M. *J. Biomed. Mater. Res.* **1999**, *44* (3), 298.
(41) Phuvanartnuruks, V.; McCarthy, T. J. *Macromolecules* **1998**, *31* (6), 1906.

BM0341834